IOSR Journal of Applied Chemistry (IOSR-JAC)
e-ISSN: 2278-5736.Volume 8, Issue 5 Ver. II (May. 2015), PP 73-84
www.iosrjournals.org

Synthesis, Structural, Spectral Characterization and DNA/Protein Binding Studies on Cobalt (II) Complex Containing Acetylacetone Ligand

S. Kadhiravan, S. Sivajiganesan,
[a]*Department of chemistry, AVVM Sri Pushpam College Poondi Thanjavur,613 503 Tamilnadu India*

Abstract: *A new cobalt(II) complex, [Co(acac)$_3$], (where, acac=acetylacetone) has been synthesized and characterized by elemental analysis, UV-Vis, FT-IR and thermal analysis and single crystal X-ray diffraction techniques. The result of characterization showed that the crystal is monoclinic system, P21/c space group with crystal parameters: a=13.8081(10)Å, b=7.4354(4)Å, c=16.1352(11) Å and Z = 4. The Co(II) had an ideal octahedral coordination environment with four oxygen atoms of acetylacetone ligand. Binding of this Co(II) complex with calf thymus DNA was investigated by UV-Visible absorption, fluorescence spectroscopy techniques. The intrinsic binding constants K_b of complex with CT-DNA obtained from UV-Vis absorption studies were 4.43 × $10^5 M^{-1}$. Further, the in vitro cytotoxic effect of the complexes examined on cancerous cell line, such as human breast cancer cells (MCF-7).*

Keywords: *Co (II) complex, Crystal structure, DNA interaction and cytotoxicity activity.*

I. Introduction

Deoxyribonucleic acid plays an important role in the life process, because it bears heritage information and instructs the biological synthesis of proteins and enzymes through the replication and transcription of genetic information in living cells. DNA is a particularly good target for metal complexes as it offers a wide variety of potential metal binding sites [1,2]. Transition metal complexes with beta-diketones are known to possess bacteriocidal. Antiviral, antifungal and antialgal activities [3]. Metal complexes having N, O donor atoms are very important because of their significant biological properties such as antibacterial, antifungal, anticancer and herbicidal [4]. Cobalt is an essential trace element in humans, exhibiting many useful biological functions. Numerous compounds, naturally occurring and man-made, contain the cobalt at two common oxidation states Co(II) and Co(III). There is growing interest in investigating cobalt and other transition metal complexes for their interaction with DNA. This may be partly influenced by the results of extensive investigation into two areas of research, viz (i) the binding specificity of small organic molecules for their possible modulation and inhibition of DNA replication, transcription and recombination, and (ii) anticancer, antiviral and antibacterial drugs [5,6]. The interest on cobalt complexes in experimental cancer therapy research results from their role as systemic anticancer agents and their ability to redox-dependent targeting the tissue of solid tumours. The former role was firstly attrubuted to the fact that vitamin B12 (cobalamin) is substituted together with folic acid in chemotherapy regimens involving antimetabolites to reduce unwanted side effects, and, secondly, to the fact that fast proliferating cells require higher amounts of vitamins B12 than normal ones [7]. Since the first reported studies into the biological activity of Co complexes [8] in 1952, diverse structurally characterized cobalt complexes showing antitumor anti-proliferative [9,10], antimicrobial [11,12], antifungal [13,14], antiviral [15,16] and antioxidant [17] activities have been reported.

Accordingly, we intend to report herein, the synthesis of Co(II) complex with acetylacetone ligand and characterization of complex was carried out by elemental analysis, IR, UV-Vis and thermal studies. The crystal structure of complex has been determined by X-ray crystallography. The binding properties of this complex to CT-DNA have been carried out using different physico-chemical methods and the binding modes are discussed.

II. Physical Measurements

Elemental analyses of carbon, hydrogen, and nitrogen were performed on a Carlorerba-1106 microanalyzer. The electronic spectra were recorded on a Shimadzu UV-3101PC spectrophotometer. FT-IR spectra were recorded in the 4000–400 cm^{-1} region using KBr pellets on a Bruker EQUINOX 55 spectrometer. The fluorescence study was carried out on an Elico SL 174 spectrofluorometer. The molar conductivity of a freshly prepared solution of the complexes (10^{-3} M) in DMF was measured using an Elico Model SX80 conductivity bridge.

2.1. X-ray crystallography

Single-crystal X-ray diffraction data of cobalt complexes were collected at 296(2) K, on a Bruker Smart 1000 CCD diffractometer using Mo-Kα radiation with the ω scan technique. An empirical absorption correction was applied to the raw intensities. The structures were solved by direct methods (SHELX- S-97) [18] and refined with full-matrix least-squares technique on F^2 using the SHELXL-97 [19]. The hydrogen atoms were added theoretically, and riding on the concerned atoms and refined with fixed thermal factors.

2.2. Absorption spectrophotometric studies

Absorption spectra titrations were performed at room temperature in Tris-HCl/NaCl buffer (50 mM Tris-HCl/1 mM NaCl buffer, pH 7.5) to investigate the binding affinity between CT-DNA and complex. 2 mL solutions of the blank Tris–HCl/NaCl buffer and the Co(II) complex sample ([complex] = 5×10^{-6} M) were placed into two 1 cm path cuvettes, respectively. Then one aliquot (10 μL) of buffered CT-DNA solution (0.01 M) was added to each cuvette in order to eliminate the absorbance of DNA itself. Before the absorption spectra were recorded, the Co(II)-DNA solutions were incubated at room temperature for 5 min in order to full reaction.

2.3. Competitive Binding Experiments

The relative binding of complexes to CT-DNA were determined with an EB-bound CT-DNA solution in Tris–HCl/NaCl buffer (pH=7.2, 5 mM Tris–HCl, 50 mM NaCl). The experiments were carried out by adding a certain amount of a solution of complexes ([complex] = 1.0×10^{-3} M) step by step into the EB–DNA solution (2.4 μM EB and 48 μM CT-DNA). The influence of the addition of complexes to the EB-DNA complex have been obtained by recording the variation of fluorescence emission spectra with excitation at 510 nm and emission at 602 nm. Before the emission spectra were recorded, the Co(II)-DNA solutions were incubated at room temperature for 5 min in order to full reaction.

2.4. Cell culture

The MCF-7 human breast cancer cell line was obtained from National Center for Cell Sciences (NCCS), Pune, India. The cell line was cultured in the Dulbecco's Modified Eagles medium (DMEM) supplemented with 10% fetal bovine serum (FBS), 200 mM L-glutamine, 100 U/mL penicillin, and 10 mg/mL streptomycin in a humidified atmosphere consisting of 5% CO_2 at 37º C.

2.5. Evaluation of cytotoxicity

The cytotoxic effect of complexes (**1-3)** against MCF-7 cells was evaluated by MTT [3-(4, 5-dimethylthiazol-2-yl)-2,5-diphenyltetrazolium bromide] assay. Briefly, MCF-7 cells were seeded (5×10^4 cells/well) in a 96-well plate and kept in CO_2 for attachment and growth for 24 h. Then, the cells were treated with various concentrations of complexes dissolved in DMSO (0.25-100 μM) and incubated for 24 h. After incubation, the culture medium was removed and 15 μL of the MTT solution (5 mg/mL in PBS) was added to each well. Following 4 h incubation in dark, MTT was discarded and DMSO (100 μL/well) was added to solubilize the purple formazan product. The experiment was carried out in triplicates and the medium without complex served as control. The absorbance was measured colorimetrically at 570 nm using an ELISA microplate reader. The percentage of cell viability was calculated using the following formula and expressed as IC_{50};

% cell viability = (OD value of treated cells)/ (OD value of untreated cells (control) ×100

The IC_{50} value is calculated using linear regression from excel.

2.6. Synthesis of complex [Co(acac)$_3$]

2.6.1. [Co(acac)$_3$] (1)

To a solution of acetylacetone (0.12 g, 1mmol) in methanol (10 ml), sodium hydroxide (0.05 g, 1mmol) was added and the resulting solution was stirred for 15 min at room temperature. $CoCl_2.6H_2O$ (0.3 g, 1mmol) in methanol (10 ml) was added to the solution. To the reaction mixture stirring for 3 h. The pink colored precipitate formed was dissolved in DMF and kept for crystallization. Five days later round-shaped brown crystals suitable for X-ray diffraction were obtained. Yield: 70 %. m.p. 226°C. Anal. Cal. (%) for C_{15} H_{21} Co O_6: C, 50.56; H, 5.89. Found (%): C, 50.30; H, 6.03. FT-IR, (ν cm-1) (KBr Disc): 3383br, 2068s, 1624s, 1591s 803s, 652s (br-broad, s-sharp). UV-vis in DMF [λ_{max}/nm (ε_{max}/ mol^{-1} cm^{-1})]: 269 (264), 293(232), 607(437), 672(698).

III. Results And Discussion

3.1. X-ray structure characterization

Perspective views of complex 1 which is formulated as [Co(acac)$_3$] are given in Fig. 1 and crystal packing diagram of complex Fig. 2. A summary of the crystal data, refinement results has been given in Table 1 and selected bond lengths and bond angles are listed in Table 2. The complex crystallizes in the monoclinic

space group P21/c. The metal ion is coordinated to the nitrogen and oxygen atoms of the 8-hq ligand and the coordination geometry around Co (II) is described as distorted octahedral. The structure show that the cobalt metal centre is octahedral with an O_6 coordination environment, as revealed by the large deviation in bond distance of $[Co(acac)_3]$ [Co(1)-O(1) - 1.8736(16), Co(1)-O(2) - 1.862(2) , Co(1)-O(3) - 1.8697(17), Co(1)-O(4) - 1.8770(19),Co(1)-O(5) - 1.8834(18), Co(1)-O(6) - 1.8751(17) and bond angles O(2)-Co(1)-O(3) – 96.91(9), O(2)-Co(1)-O(1) – 86.85(9), O(3)-Co(1)-O(1) – 174.90 (8) , O(2)-Co(1)-O(6) – 88.95(8), O(3)-Co(1)-O(6) – 87.08(8), O(1)-Co(1)-O(6) - 96.47(7), O(2)-Co(1)-O(4) - 96.47(7), O(3)-Co(1)-O(4) – 88.32(8), O(1)-Co(1)-O(4) - 88.16(8), O(6)-Co(1)-O(4) - 87.62(8), O(2)-Co(1)-O(5) - 87.65(8), O(3)-Co(1)- O(5) - 88.51(8), O(1)-Co(1)-O(5) - 88.20(7), O(6)-Co(1)-O(5) – 174.07(8) and O(4)-Co(1)-O(5) – 96.21 (8) from the ideal angle for 90°.

3.2. IR and UV/vis spectroscopy

There are conspicuous differences between the complex and free ligand in IR spectrum [20]. In the free ligand amedium-intensity band at 3383 cm^{-1}, assigned to υ(OH) of diketone tautomer, and two strong bands around 1624 and 1591 cm^{-1}, due to (C O) of the lateral chain and (C O) of pyrazolone ring respectively, are absent in the complex [21]. In the complex, there are four new bands at 2068 cm^{-1}, 1624 cm^{-1} and 652 cm^{-1}, respectively, assigned to [υ(C—O−)], υ(C C C), water molecules [22] and Co—O, respectively (Fig. 3).

UV–vis absorption spectra of complex in ethanolic solutionwere recorded in thewavelength range 200–800 nm. Two absorptions of the complex at 269, 293 nm are attributed to л–л* transitions of aryl ring, carbonyl, and n–л* transition of carbonyl [23]. In the visible region, weaker absorptions near 607 and 672 nm for the Co(II) complex are assigned as $4T_1g \rightarrow 4A_2g$, $4T_1g \rightarrow 4T_2g$ (F) for d–d transitions, consistentwith Co in an octahedral environment (Fig. 4).

3.3. Thermal studies

Thermogravimetric (TG) and differential thermogravimetric (DTA) analysis (Fig.5) were carried out for the complex 1 under nitrogen flow at the constant heating of 10°C per minute. The thermogram of this complex decomposition observed in the range 100-200°C (50% corresponds to the weight loss acetylacetone moiety present in the complex 1. There are four DTA endotherm peak observed at 55.85, 86.08, 138.09 and 168.79°C, respectively, also confirmed the decomposition and weight loss of ligand moieties. The residue left in the crucible consists of corresponding metal oxide [24].

3.4. DNA binding studies

3.4.1. Study of the interaction of the complexes with CT DNA with UV spectroscopy

Transition metal complexes can bind to DNA via both covalent (via replacement of a labile ligand of the complex by a nitrogen base of DNA) and/or noncovalent (intercalation, electrostatic or groove binding) interactions [25]. In the literature, metal complexes has been found to bind to DNA via the intercalative mode [26]. The UV spectra have been recorded for a constant CT DNA concentration in different [complex]/[DNA] mixing ratios. UV spectra of CT DNA in the presence of a compound derived for diverse r values are shown representatively for Fig. 6. The band at λmax = 258 nm exhibits a red-shift up to 2 nm for all compounds, indicating that the interaction with CT DNA results in the direct formation of a new complex with double-helical CT DNA [27] with a simultaneous stabilization of the CT DNA duplex [28]. In the UV spectra of the complex, the intense absorption bands observed are attributed to the intra-ligand transitions of the coordinated groups of acetylacetone ligands. Any interaction between complex and CT DNA that could perturb its intraligand centred spectral transitions during the titration upon addition of CT DNA in diverse r values can be observed [29]. In general, the changes observed in the UV spectra upon titration may give evidence of the existing interaction mode, since a hypochromism due to π-π* stacking interactions may appear in the case of the intercalative binding mode, while red-shift (bathochromism) may be observed when the DNA duplex is stabilized [26]. According to linear Stern-Volmer equation: [25],

$$I_0/I=1+K_{sv}r,$$

where I_0 and I are the fluorescence intensities in the absence and the presence of complex. K_{sv} is a linear Stern-Volmer quenching constant, r is the ratio of the total concentration of complex to that of DNA. The quenching plot illustrates that the quenching of EB bound to DNA by the complexes is in good agreement with the linear Stern-Volmer equation, which also indicated that the complexes binds to DNA. In the plot of I_0/I versus [Complex]/[DNA], K_{sv} is given by the ratio of the slope to intercept. The K_{sv} value for our complex thus obtained is $4.43 \times 10^5\ M^{-1}$, respectively. This may suggest that the complex **1** has intercalative mode of binding that involves a stacking interaction between the complexes and the base pairs of DNA.

3.4.2. Competitive study with ethidium bromide

Ethidium bromide (EB) is a typical indicator of intercalation since it can form soluble complexes with nucleic acids resulting in the emission of intense fluorescence due to the intercalation of the planar phenanthridine ring between adjacent base pairs on the double helix of CT DNA. The changes observed in the spectra of EB on its binding to CT DNA are often used for the interaction study between DNA and metal complex [30]. Complex **1** shows no fluorescence at room temperature in solution or in the presence of CT DNA, and their binding to DNA cannot be directly predicted through the emission spectra (Fig. 7). Hence competitive EB binding studies may be undertaken in order to examine the binding of each compound with DNA since the fluorescence intensity is highly enhanced upon addition of CT DNA, due to its strong intercalation with DNA base pairs. Addition of a second molecule, which may bind to DNA more strongly than EB, results in a decrease the DNA-induced EB emission due to the replacement of EB, and/or electron transfer [31,32].

The emission spectra of EB bound to CT DNA in the absence and presence of each compound have been recorded for [EB] = 20 mM, [DNA] = 26 mM for increasing amounts of each compound. The addition of complex **1** at diverse r values (Fig. 6) results in a significant decrease of the intensity of the emission band of the DNA-EB system at 592 nm indicating the competition of the complex with EB in binding to DNA. The observed significant quenching of DNA-EB fluorescence for complex **1** suggests that they displace EB from the DNA-EB complex **1** and they can probably interact with CT DNA by the intercalative mode [33]. The Stern-Volmer constant K_{sv} may be used to evaluate the quenching efficiency for each compound according to the equation:

$$I_0/I=1+K_{sv}r,$$

where I_0 and I are the emission intensities in the absence and the presence of the quencher, respectively, [Q] is the concentration of the quencher and K_{sv} is obtained by the slope of the diagram I_0/I vs [Q]. The K_{sv} value for our complex thus obtained is 3.9×10^4 M^{-1}, respectively. The Stern-Volmer plots of DNA-EB for the compounds illustrate that the quenching of EB bound to DNA by the compounds is in good agreement (R = 0.9983) with the linear SterneVolmer equation, which proves that the replacement of EB bound to DNA by each compound results in a decrease in the fluorescence intensity.

3.4.3. Circular dichroism

CD spectroscopic technique can be successfully utilized to detect the conformational changes of DNA induced by its interaction with metal complex. The CD spectrum of CT-DNA was recorded in the range 220–320 nm in 0.1 M phosphate buffer (pH 7.2) and it has been found that there were one positive band at 275 nm due to base stacking and one negative band at 245 nm due to helicity [34]. The examination of Fig. 8 indicates that the positive band slightly increased in intensity and the negative band decreased in intensity after the binding of complex with DNA however no considerable shift in λmax could be observed. A very small decrease in the intensity of positive band and a small increase in the intensity of negative band were observed when the DNA. Intercalation binding interaction of the complex with DNA have been shown to bring about only marginal changes in the intensity of negative band as well as the positive band of DNA and no significant shift observed positive and negative band.

3.4.4. Interaction of the complexes with serum albumin proteins

It is important to consider the interactions of drugs with blood plasma proteins particularly with serum albumin, which is the most abundant protein in plasma and is involved in the transport of metal ions and metal complex with drugs through the blood stream. Binding to these proteins may lead to loss or enhancement of the biological properties of the original drug, or provide paths for drug transportation [35]. Bovine serum albumin (BSA) is the most extensively studied serum albumin, due to its structural homology with human serum albumin (HSA). BSA (containing two tryptophans, Trp-134 and Trp-212) solutions exhibit a strong fluorescence emission with a peak at 343 nm, respectively, due to the tryptophan residues, when excited at 295 nm [36]. The interaction of complex **1** with serum albumins has been studied from tryptophan emission-quenching experiments. The changes in the emission spectra of tryptophan in BSA are primarily due to change in protein conformation, subunit association, substrate binding or denaturation. Complexes **1** exhibited a maximum emission at 355 nm (Fig. 9) under the same experimental conditions and the SA fluorescence spectra have been corrected before the experimental data processing [37]. Addition of complex **1** to BSA results in relatively low fluorescence quenching (Fig. 10**),** due to possible changes in protein secondary structure of BSA indicates the binding of the compounds to BSA [38]. The Stern–Volmer and Scatchard graphs may be used in order to study the interaction of a quencher with serum albumins. According to Stern–Volmer quenching equation [37,39]:

$$\frac{I_0}{I} = 1 + k_q \tau_0 [Q] = 1 + K_{SV} [Q]$$

where I_0 = the initial tryptophan fluorescence intensity of SA, I = the tryptophan fluorescence intensity of SA after the addition of the quencher, k_q = the quenching rate constants of SA, K_{sv} = the dynamic quenching constant, τ_0 = the average lifetime of SA without the quencher, [Q] = the concentration of the quencher respectively,

$$K_{sv} = k_q \tau_0$$

and, taking as fluorescence lifetime (τ_0) of tryptophan in SA at around 10^{-8}s, the dynamic quenching constant (K_{sv}, M^{-1}) can be obtained by the slope of the diagram I_0/I vs [Q] (Fig. 11), and subsequently the approximate quenching constant (k_q, M^{-1} s^{-1}) may be calculated. The calculated values of K_{sv} and k_q for the interaction of the compounds with BSA are given in Table 3 and indicate a good BSA binding propensity of the complex exhibiting the highest BSA quenching ability. The k_q values are higher than diverse kinds of quenchers the existence of a static quenching mechanism [40, 41]. Using the Scatchard equation [37]:

$$\frac{\Delta I/I_0}{[Q]} = nK - K\left(\frac{\Delta I}{I_0}\right)$$

where n is the number of binding sites per albumin and K is the association binding constant, K (M^{-1}), may be calculated from the slope in plots ($\Delta I_0/I$)/[Q] versus ($\Delta I/I_0$) (Fig. 12) and n is given by the ratio of the y intercept to the slope. The K values of the complexes (**1-3**) for albumins, being in the value given Table 3. The Stern-Volmer equation applied for the interaction with BSA in Fig. 12 shows that the curves have fine linear relationships (r = 0.9921). The calculated values of K_{sv}, n and k_q are given in Table 3 and indicate their good BSA binding propensity with complexes**.** From the Scatchard graph (Fig. 11), the association binding constant to BSA of each compound has been calculated (Table 3) with complex **2** exhibiting higher K values than other complexes. Therefore, the study of the binding to albumins may reveal useful information concerning future application.

3.8. Cytotoxic activity

Cytotoxic potential of newly synthesized complex **1** was investigated on human breast cancer cell (MCF-7). The complex **1** were applied in range of concentration 0.25-100 µM for MCF-7 and left for 48 h. The activities of the complexes were determined by MTT test in vitro and the results were expressed in terms of IC_{50} values. The relations of inhibition rates and complexes concentrations against human breast cancer cell (MCF-7) were shown in Fig.13. The inhibition effects were further enhanced by increasing the concentration of complexes. At the concentration of 100 µM, inhibition rates of the complex **1** against human breast cancer cells reached nearly same values. The values of IC_{50} for the complex **1** were >100 µM. It is commonly believed that the biological activities of anticancer metal complex are dependent on their ability to bind DNA and damage its structure resulting in the impairment of its function, which is followed by inhibition of replication, transcription processes and eventually cell death, if the DNA lesions are not properly repaired. The type of metal ion may be another reason for their different anticancer activity [42]. This is due to the fact that cobalt complexes have the capacity to reduce the energy status in tumors, as well as to enhance tumor hypoxia, which also influences their antitumor activities.

IV. Conclusions

The complex [$Co(acac)_3$] has been synthesized and characterized. Molecular structure of complex **1** was determined by X-ray crystallography afforded elongated octahedral coordination geometry. Complex **1** bind to CT DNA through intercalative binding mode. The complex shows good binding affinity to BSA proteins and to give relatively high binding constant. The in vitro cytotoxicity study on breast cancer cell line (MCF-7) indicates that complex has the potential to act as effective anticancer drug. These studies form an important rationale for drug design and warrant further in vivo experiments and pharmacological assays.

Acknowledgement

The authors thank the STIC Cochin University of Technology, Cochin-682 022, Kerala for single crystal X-ray diffraction analysis of the complexes.

Figure Captions:

Fig. 1. OPTEP views of the molecular structure and atom labeling scheme of complex **1**.
Fig. 2. Crystal packing diagram of complex **1**.
Fig. 3. FT-IR analysis of complex **1**.
Fig.4. UV-Vis analysis of complex **1**.
Fig.5. Thermal analysis of complex **1**.

Fig. 6. Absorption spectra of complex **1** in 5 mM Tris-HCl/buffer upon addition of DNA. The inner plot of [DNA/(ε_a-ε_f) vs [DNA] for the titration of DNA with complex
Fig. 7. Fluorescence emission spectra of the EB-DNA in presence of complex 1 in 5mM Tris HCl buffer (pH 7.2). The inner plot of [I_0/I] vs complex concentration.
Fig. 8. CD spectra of CT-DNA (1.0 x 10^{-4} M), and the interaction with complex **1** ([complex]/[DNA] = 0.5). All the spectra were recorded in 5 mM Tris–HCl/ 50 mM NaCl buffer, pH 7.2 and 25 °C.
Fig.9. Fluorescence spectra of BSA in presence of various concentration of complex **1**.
Fig.10. Plot of % relative fluorescence intensity at λ_{em} = 355 nm (I/I_0 (%)) vs r (r = [compound]/[BSA]) for complex **1** in buffer solution (pH 7.0).
Fig. 11. Fluorescence spectra of BSA in emission intensity I_0/I vs [Q]. [Q = complex]
Fig.12. Determination of the complex-BSA binding constant and the number of binding sites of BSA.
Fig. 13. Cytotoxic effect of complexes (**1-3**) against MCF-7 at different concentration. Cell viability decreased with increasing concentration of complex **1**.

Reference

[1]. A.M. Pyle, E.C. Long, J.K. Barton, J. Am. Chem. Soc. 111 (1989) 4520.
[2]. A. Sitlani, E.C. Long, A.M. Pyle, J.K. Barton, J. Am. Chem. Soc. 114 (1992) 2303.
[3]. F. P. Dwyer, E. C. Gyarfas, W. B. Rogers and J. H. Koch, Nature, 170,190 (1952).
[4]. J. M. Lazić, L. Vučićević, S. Grgurić-Šipka, K. Janjetović, G.N. Kaluđerović, M. Misirkić, M.G. Pavlović, D. Popadić , R. Paschke, V. Trajković , T.J. Sabo, ChemMedChem. 5 (2010) 881.
[5]. A.D. Richards, A. Rodger, Chem. Soc. Rev. 36 (2007) 471–483.
[6]. B.M. Zeglis, V.C. Pierre, J.K. Barton, Chem. Commun. (2007) 4565–4579.
[7]. T.F.S. Silva, L.M.D.R.S. Martins, M.F.C. Guedes da Silva, A.R. Fernandes, A. Silva, P.M. Borralho, S. Santos, C.M.P. Rodrigues, A.J.L. Pombeiro, Dalton Trans. 41 (2012) 12888-12897.
[8]. M.D. Hall, T.W. Failes, N. Yamamoto, T.W. Hambley, Dalton Trans. (2007) 3983–3990.
[9]. H. Lopez-Sandoval, M.E. Londono-Lemos, R. Garza-Velasco, I. Poblano-Melendez, P. Granada-Macias, I. Gracia-Mora, N. Barba-Behrens, J. Inorg. Biochem. 102 (2008) 1267–1276.
[10]. I. Ott, A. Abraham, P. Schumacher, H. Shorafa, G. Gastl, R. Gust, B. Kircher, J. Inorg.Biochem. 100 (2006) 1903–1906.
[11]. D.U. Miodragovic, G.A. Bogdanovic, Z.M. Miodragovic, M.D. Radulovic, S.B. Novakovic, G.N. Kaludjerovic, H. Kozlowski, J. Inorg. Biochem. 100 (2006) 1568–1574.
[12]. K. Nomiya, A. Yoshizawa, K. Tsukagoshi, N.C. Kasuga, S. Hirakawa, J. Watanabe, J. Inorg. Biochem. 98 (2004) 46–60.
[13]. J. Lv, T. Liu, S. Cai, X. Wang, L. Liu, Y. Wang, J. Inorg. Biochem. 100 (2006) 1888–1896.
[14]. Z. Weiqun, Y. Wen, X. Liqun, C. Xianchen, J. Inorg. Biochem. 99 (2005) 1314–1319.
[15]. A. Bottcher, T. Takeuchi, K.I. Hardcastle, T.J. Meade, H.B. Gray, Inorg. Chem. 36 (1997) 2498–2504.
[16]. T. Takeuchi, A. Bottcher, C.M. Quezada, T.J. Meade, H.B. Gray, Bioorg. Med. Chem. 7 (1999) 815–819.
[17]. F. Dimiza, A.N. Papadopoulos, V. Tangoulis, V. Psycharis, C.P. Raptopoulou, D.P. Kessissoglou, G. Psomas, Dalton Trans. 39 (2010) 4517–4528.
[18]. G. M. Sheldrick, SHELXS-97, Program for the Solution of Crystal Structures, University of Göttingen, Germany, 1997.
[19]. G. M. Sheldrick, SHELXL-97, Program for the Refinement of Crystal Structures, University of Göttingen, Germany, 1997.
[20]. The infrared spectrum was recorded from a KBr flake by use of a Perkin Elmer FTIR-1730 spectrometer.
[21]. E.C. Okafor, Spectrochim. Acta Part A 37 (1981) 945.
[22]. M.M. Zhang, P.F. Li, J. Inorg. Chem. 4 (2004) 440.
[23]. A.B.P. Lever, Inorganic Electronic Spectroscopy, Elsevier, Amsterdam, 1984.
[24]. J. Cernak, J.Chonic, J. Thermal Anal. 32 (1987) 527-532.
[25]. F. Dimiza, A.N. Papadopoulos, V. Tangoulis, V. Psycharis, C.P. Raptopoulou, D.P. Kessissoglou, G. Psomas, Dalton Trans. 39 (2010) 4517-4528.
[26]. A.M. Pyle, J.P. Rehmann, R. Meshoyrer, C.V. Kumar, N.J. Turro, J.K. Barton, J. Am. Chem. Soc. 111 (1989) 3053-3063.
[27]. S. Fountoulaki, F. Perdih, I. Turel, D.P. Kessissoglou, G. Psomas, J. Inorg. Biochem. 105 (2011) 1645-1655.
[28]. P. Christofis, M. Katsarou, A. Papakyriakou, Y. Sanakis, N. Katsaros, G. Psomas, J. Inorg. Biochem. 99 (2005) 2197-2210.
[29]. S. Roy, R. Banerjee, M. Sarkar, J. Inorg. Biochem. 100 (2006) 1320-1331.
[30]. F. Dimiza, A.N. Papadopoulos, V. Tangoulis, V. Psycharis, C.P. Raptopoulou, D.P. Kessissoglou, G. Psomas, Dalton Trans. 39 (2010) 4517-4528.
[31]. A. Tarushi, G. Psomas, C.P. Raptopoulou, D.P. Kessissoglou, J. Inorg. Biochem. 103 (2009) 898e905.
[32]. K.C. Skyrianou, F. Perdih, I. Turel, D.P. Kessissoglou, G. Psomas, J. Inorg. Biochem. 104 (2010) 740-749.
[33]. K.C. Skyrianou, V. Psycharis, C.P. Raptopoulou, D.P. Kessissoglou, G. Psomas, J. Inorg. Biochem. 105 (2011) 63-74.
[34]. A.M. Polyanichko, V.V. Andrushchenko, E.V. Chikhirzhina, V. Vorobev, H. Wieser, Nucleic Acids Res. 32 (2004) 989-996.
[35]. C. Tan, J. Liu, H. Li, W. Zheng, S. Shi, L. Chen, L. Ji, J. Inorg. Biochem. 102 (2008) 347–358.
[36]. Y. Wang, H. Zhang, G. Zhang, W. Tao, S. Tang, J. Lumin. 126 (2007) 211–218.
[37]. F. Dimiza, F. Perdih, V. Tangoulis, I. Turel, D.P. Kessissoglou, G. Psomas, J. Inorg. Biochem. 105 (2011) 476–489.
[38]. V. Rajendiran, R. Karthik, M. Palaniandavar, H. Stoeckli-Evans, V.S. Periasamy, M.A. Akbarsha, B.S. Srinag, H. Krishnamurthy, Inorg. Chem. 46 (2007) 8208–8221.
[39]. F. Dimiza, A.N. Papadopoulos, V. Tangoulis, V. Psycharis, C.P. Raptopoulou, D.P. Kessissoglou, G. Psomas, Dalton Trans. 39 (2010) 4517–4528.
[40]. I. Bertini, C. Luchinat, in: G.L. Eichorn, L.G. Marzilli (Eds.), Advances in Inorganic Biochemistry, vol. 6, Elsevier, New York, 1984, pp. 78–80.
[41]. G.M. Sheldrick, SHELXL-97: Crystal Structure Refinement Program, University of Göttingen, Germany, 1997
[42]. S. Amer, N. El-Wakiel, H. El-Ghamry, J. Mol. Struct. 1049 (2013) 326–335.

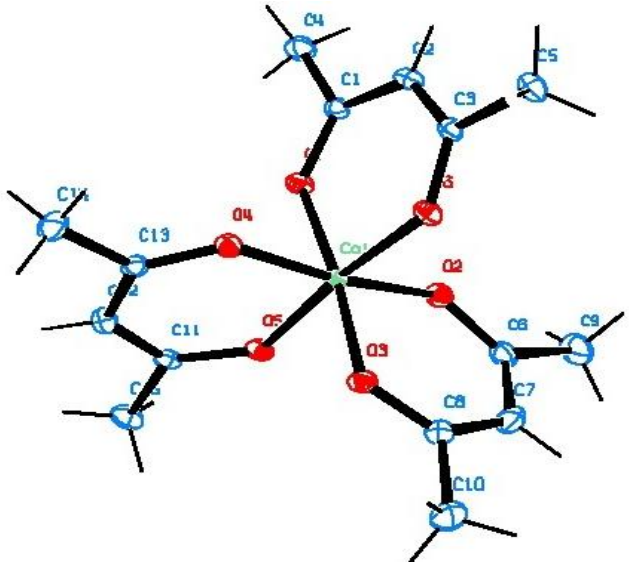

Fig. 1.

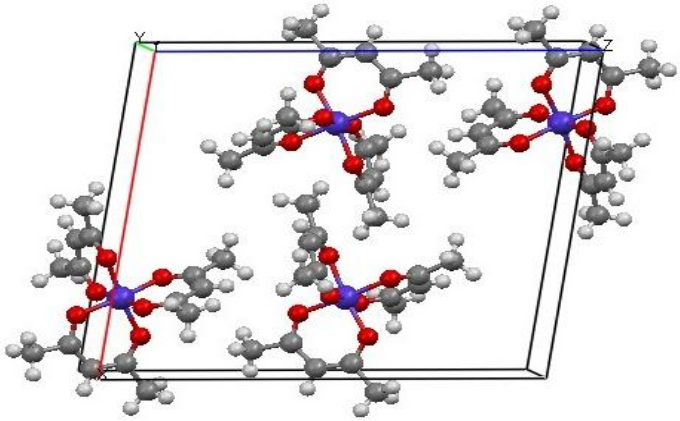

Fig. 2.

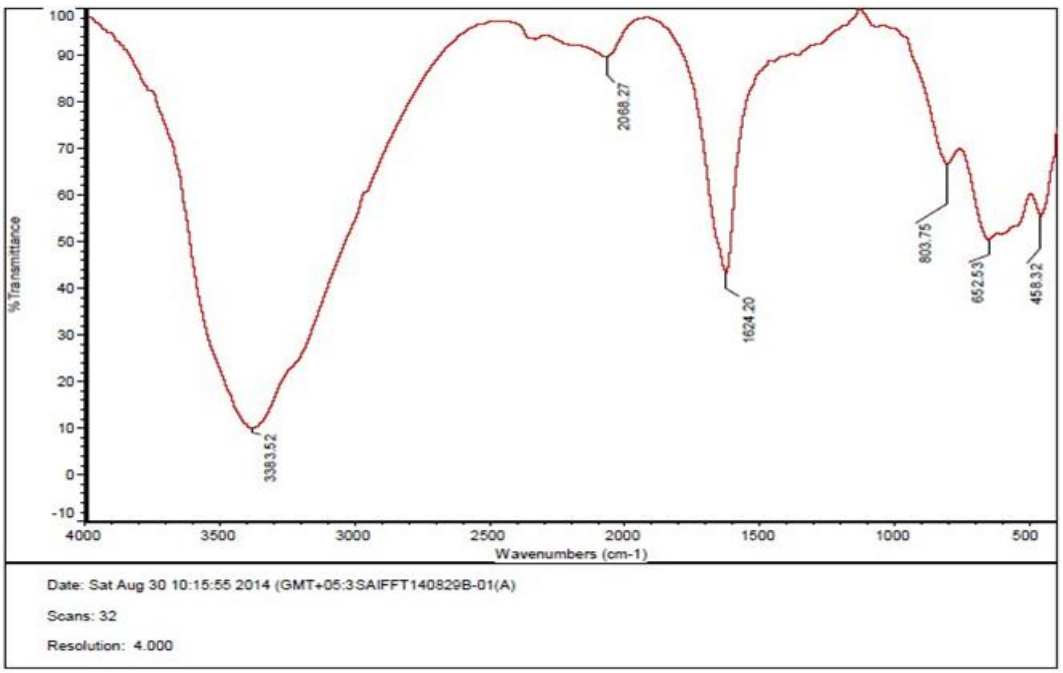

Fig. 3.

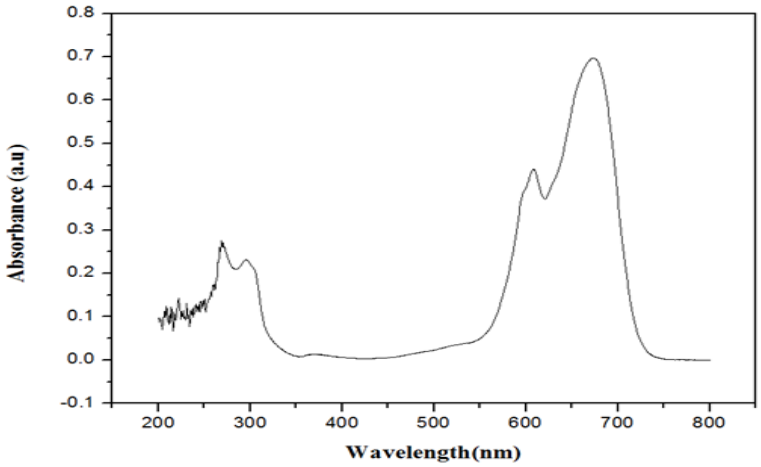

Fig.4.

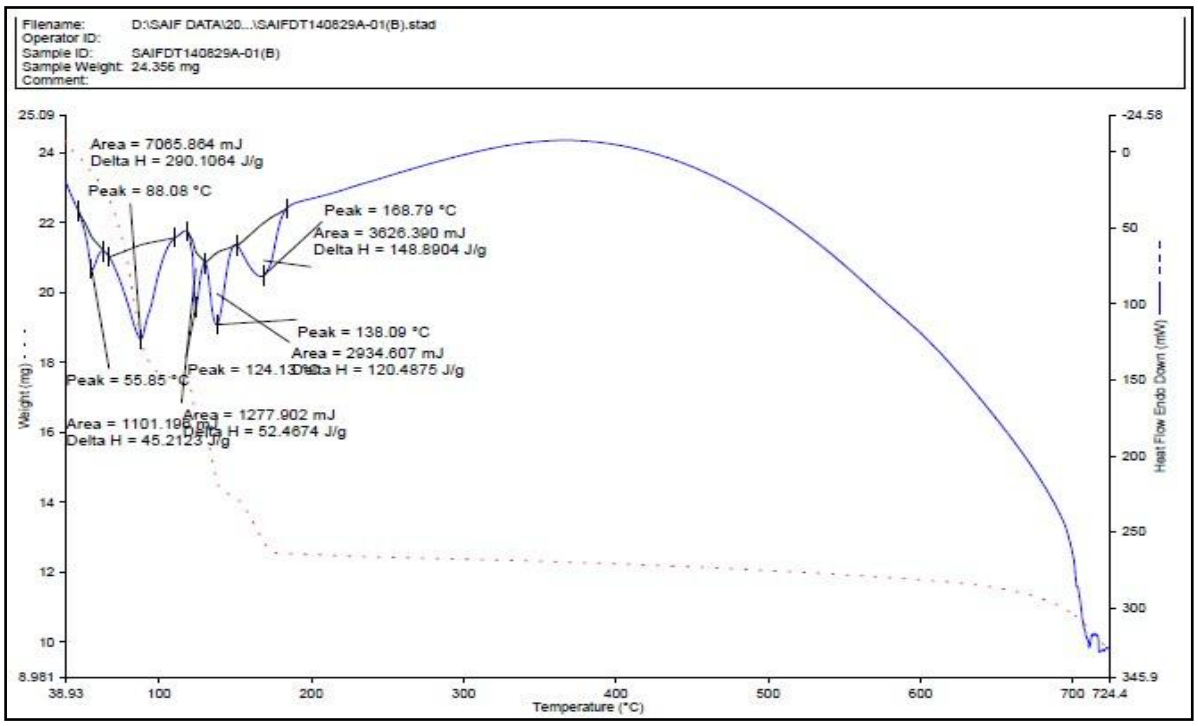

Fig.5.

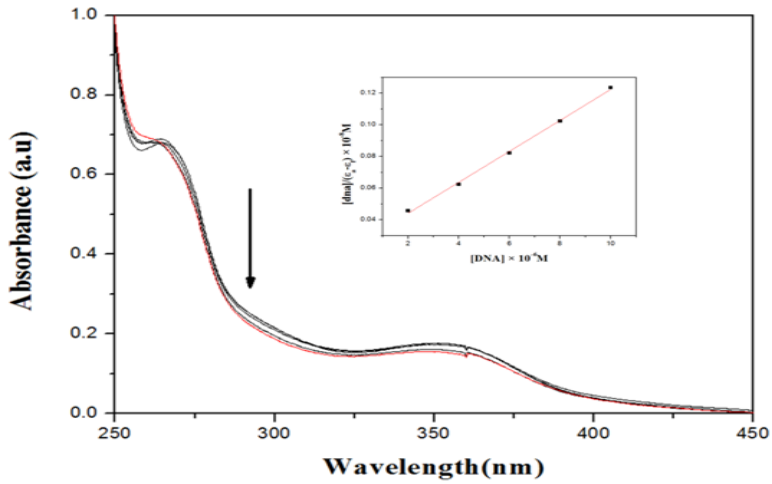

Fig. 6.

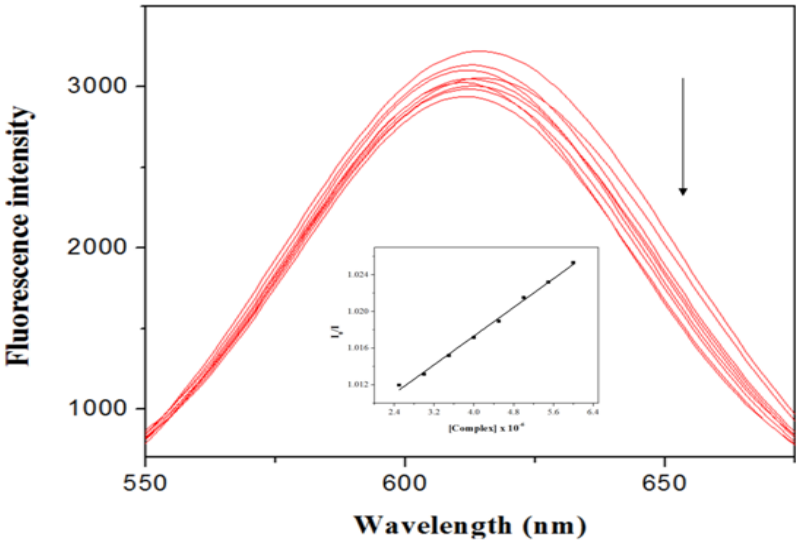

Fig. 7.

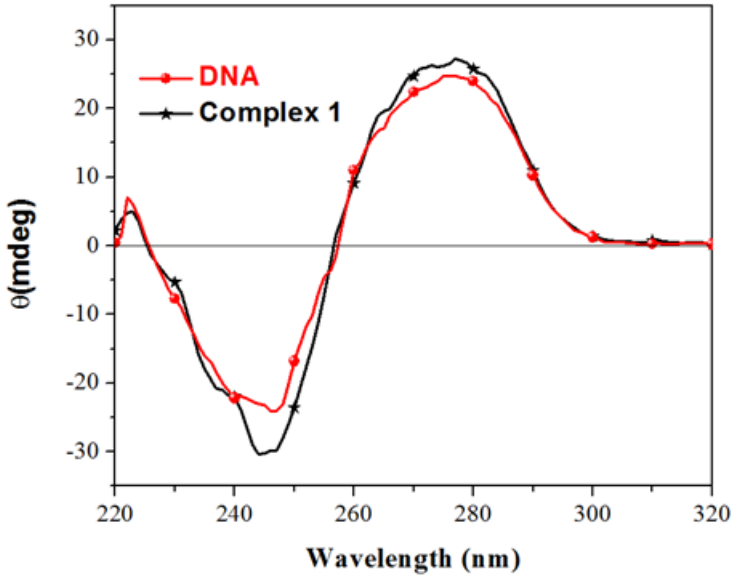

Fig. 8.

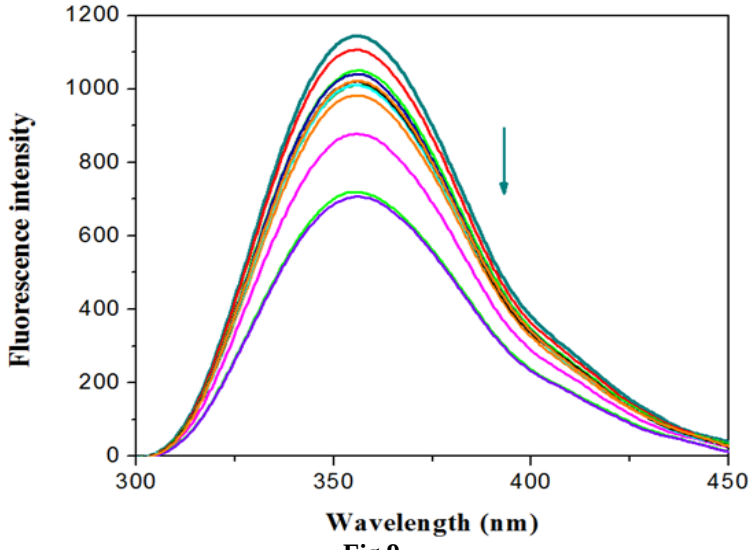

Fig.9.

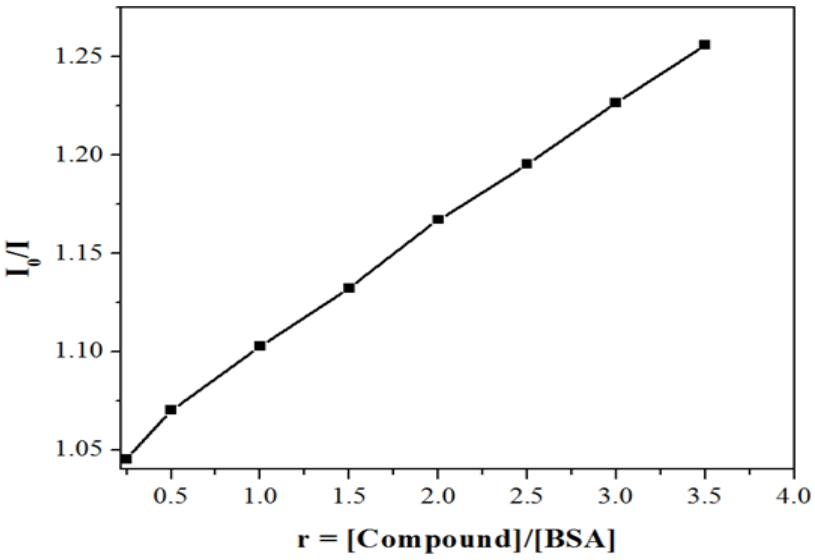

Fig.10.

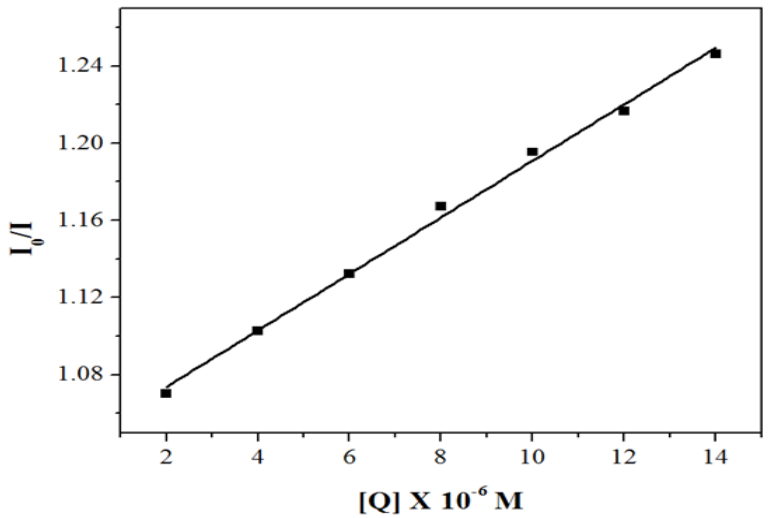

Fig.11.

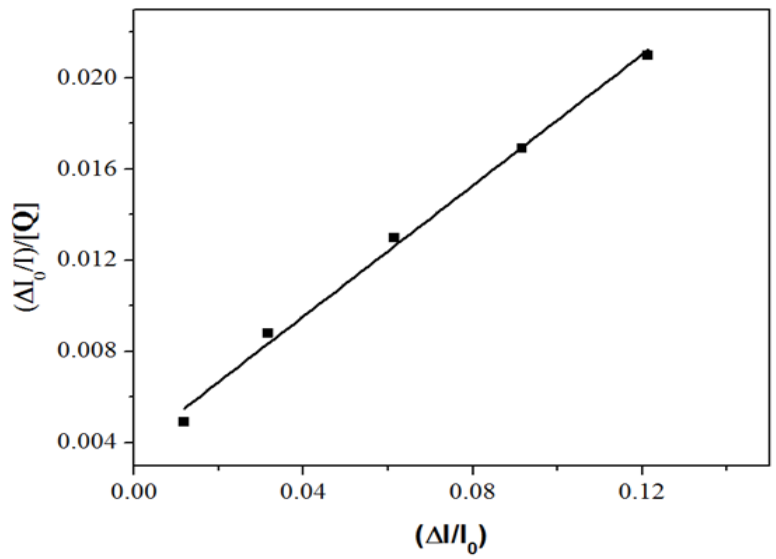

Fig.12.

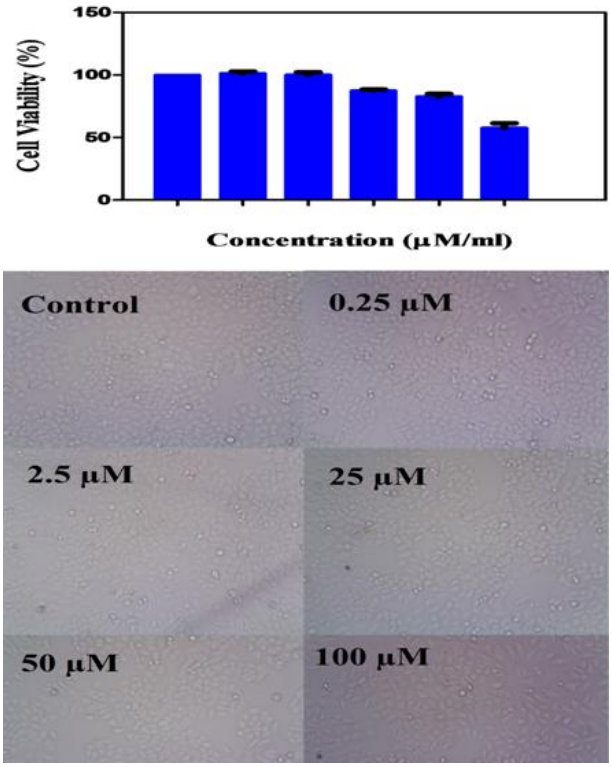

Fig.13.

Table 1. Crystallographic data and structure refinement parameters for complex

Complex	$[Co(acac)_3]$
Empirical formula	$C_{15}\ H_{21}\ Co\ O_6$
Formula weight	356.25
Temperature	296(2) K
Wavelength	0.71073 A
Crystal system	Monoclinic
space group	P21/c
a	13.8081(10) A
b	7.4354(4) A
c	16.1352(11) A
alpha	90 deg
beta	98.485(4) deg
gamma	90 deg
Volume	1638.45(19) A^{-3}
Z	4
Calculated density	1.444 Mg/m^{-3}
Absorption coefficient	1.072 mm^{-1}
F(000)	744
Crystal size	0.40 x 0.25 x 0.25 mm
Theta range for data collection	1.49 to 28.35 deg
Limiting indices	-18<=h<=16, -9<=k<=9, -21<=l<=21
Reflections collected / unique	13440 / 4036 [R(int) = 0.0329]
Completeness to theta	28.35 98.7 %
Max. and min. transmission	0.7754 and 0.6738
Goodness-of-fit on F^{-2}	1.036
Final R indices [I>2sigma(I)]	R1 = 0.0415, wR2 = 0.1064
R indices (all data)	R1 = 0.0676, wR2 = 0.1292
Largest diff. peak and hole	0.448 and -0.505 $e.A^{-3}$

Table 2. Selected Bond lengths (Å) and Bond Angles (°) for complex 1.

Bond Distance (Å)		Bond Angles (°)	
O(1)-Co(1)	1.8736(16)	O(2)-Co(1)-O(3)	96.91(9)
O(2)-Co(1)	1.862(2)	O(2)-Co(1)-O(1)	86.85(9)
O(3)-Co(1)	1.8697(17)	O(3)-Co(1)-O(1)	174.90(8)
O(4)-Co(1)	1.8770(19)	O(2)-Co(1)-O(6)	88.95(8)
O(5)-Co(1)	1.8834(18)	O(3)-Co(1)-O(6)	87.08(8)
O(6)-Co(1)	1.8751(17)	O(1)-Co(1)-O(6)	96.47(7)
		O(2)-Co(1)-O(4)	96.47(7)
		O(3)-Co(1)-O(4)	88.32(8)
		O(1)-Co(1)-O(4)	88.16(8)
		O(6)-Co(1)-O(4)	87.62(8)
		O(2)-Co(1)-O(5)	87.65(8)
		O(3)-Co(1)-O(5)	88.51(8)
		O(1)-Co(1)-O(5)	88.20(7)
		O(6)-Co(1)-O(5)	174.07(8)
		O(4)-Co(1)-O(5)	96.21(8)

Table 3. The BSA binding constant and parameters (K_{sv}, k_q, K, n and r) derived for complex **1**.

Compound	$K_{sv}(M^{-1})$	$k_q(M^{-1}s^{-1})$	$K(M^{-1})$	n	r
Complex **1**	5.5×10^4	5.5×10^{12}	0.0845	0.0932	0.9921